Anthropomorphic Finger Mechanism with a Nonelastic Bifurcate Tendon

Kazuya Yanagisawa, Shouhei Shirafuji, Shuhei Ikemoto, Koh Hosoda *

Information Science and Technology, Osaka University
yanagisawa.kazuya@ist.osaka-u.ac.jp

Abstract. To realize both grasping stability and manipulation dexterity is a central problem in development of robot hands. In recent years, many underactuated robot hands have been developed to flexibly conform to an object's surface with a simple control system. In contrast, it is difficult to realize dexterous manipulation which requires to control all degrees of freedom (DOFs). In this research, we develop a robot gripper consists of two tendon-driven robotic fingers with nonelastic bifurcate tendons to overcome the problem to realize dexterous manipulation by simple mechanism and control. The bifurcate tendon indicates a tendon which branches and connect an actuator to different links. In particular, we focus on the nonelastic bifurcate tendon that connects an actuator to links of two DOFs robotic finger. In this robotic finger, the displacement angles of the two joins are coupled by the nonelastic bifurcate tendon in the situation where no external force is exerted. If a certain amount of external force is applied on the fingertip, the bifurcate tendon can be slack and the coupling between two joints is broken. This means that the two DOFs robotic finger is easily controlled as one DOF mechanism in reaching to an object, but it can still move by releasing the coupling provided by the bifurcate tendon while the fingertip is fixed on the object. Based on this idea, we develop and control the two DOFs robotic finger that equipes two tendons including the nonelastic bifurcate tendon. In addition, we analyse the condition, where the bifurcate tendon gets slack, and confirmed in an experiment. As the result, the availability of controlling the slack of bifurcated tendon was successfully confirmed.

1 Introduction

Robot hands have been intensively studied to achieve humanlike stability and dexterity in object manipulations. During object manipulation, because a robot's body has to be controlled at the same time as the control of the hand, to simplify the control to reduce consumption of compuational resource is important. There are two types of robot hands, which are to actuate joins by motors implemented in the joints and to drive joints through tendons by pulling them, in terms of hardware designs. In development of anthropomorphic robot hands, because to implement many motors in each joints is space-consuming, the

* This work was supported by JSPS KAKENHI Grant Numbers 23650098, 24-3541.

tendon-driven mechanism has been often employed. For instance, JPL/Stanford Hand[1], Utah/MIT Hand[2], and DLR-Hand[3] are all employing the tendon-driven mechanism. In particular, ACT Hand[4] has the musculotendinous structure which is very similar with that of humans. Generally speaking, to realize dexterous object manipuation, robot hands with many degrees of freedom (DOFs) is necessary. In order for these tendon-driven hands to this end, however, many tendons more than the number of joins (i.e. the number of DOFs) have to be controlled. Therefore, the number of actuators that the tendon-driven hands needs is more than that of hands driven by motors implemented in each joints, and the control becomes complex and difficult as the number of DOFs increases.

To overcome this problem, the underactuated mechanism, which drives joints by less number of actuators, has been researched[5]. For instance, Soft Gripper realized flexible encapsulation grasping[6] and 100G Hand accomplished fast catching task[7]. In these hands, to employ passive mechanical elements such as springs instead of actuators successfully simplify their structures and controllers. Furthermore, passive mechanical elements are used to contribute flexible grasping of an object by making the contact soft. On the other hand, TUAT/Karlsruhe Hand, which has five underactuated fingers consist of rigid linckages, realizes various types of grasping[8]. In contrast with these superior outcomes, however, underactuated hands are often designed to be specialized for specific tasks, and the mechanisms are difficult to achieve generality. For example, passive mechanical elements provide flexible object grasping, but tasks such as in-hand manipulation, which require accurate position control of fingertips, becomes difficult.

Shirafuji et al. focused on the fact that the common digital extensor tendon in a human hand branches before the PIP joint to propose a mechanism for addressing the aforementioned problem, and developed the 3DOFs robotic finger with the bifurcate tendon structure[9]. Since the bifurcate tendon is nonelastic, these branches connected to different linckages are always tight, the geometric constraint provides complete coupling of these two joints, and the 3DOFs structure can be controlled as the 2DOFs mechanism. In addition, in the condition where the fingertip touching to an object receives a certain amount of external force, the coupling disappears by making one of the branches slack. Therefore, the finger controlled as the 2DOFs mechanism gets back in the original 3DOFs structure thanks to the external force. As the result, they have shown that the structure with the nonelastic bifurcate tendon can implicitly changes its DOF configuration.

The idea of the nonelastic bifurcate tendon is thought of as applicable for robot hands which are dexterous and easy to control. However, it is still not fully clarified how large external force and tensions of tendons conduce the changes in the configuration, and how the mechanism is applicable for object manipulation tasks. Therefore, it is necessary to investigate the advantages of the mechanism by developing a simple robot hand exploiting the nonelastic bifurcate tendon. So far, Sawada et al. has studied this kind of mechanism in terms of position and stiffness of a robot arm Their mechanism, however, employed elastic bifurcate tendon and did not considered slack of the branch.

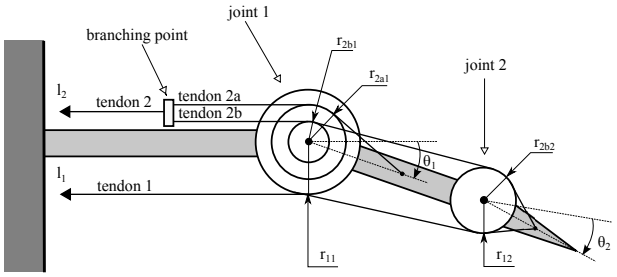

Fig. 1. Robotic finger with 2-DoFs and two tendons. One of the tendons branches at the branching point.

In this research, we develop a robot gripper consisting of 2DOFs fingers with nonelastic bifurcate tendons to realize both stable grasping and dexterous manipulation. In this paper, at first, the developed 2DOFs finger and its position control is presented. In addition, we analytically investigate the condiion, where one of branches of nonelastic bifurcate tendon looses, and confirm the validity. In the next, the robot gripper is developed by placing two developed finger. When these fingers are controlled by the same control signal, the simplest robot gripper, which two fingertips similary move on sole possible trajectory, is realized. In this design, the gripper simply opens/closes its fingers as 1DOFs mechanism until stable grasping achieved, but the postures of fingers can be changed for object manipulation by releasing fixed DOF.

2 Kinematics of Manipulator with Non-stretch Branching Tendon

Fig. 1 shows the schematic illustration of the proposed robotic finger. The finger has two DoFs and two tendons noted as tendon 1 and tendon 2. We assume that these tendons has no elasticity. Tendon 2 is branched into two different routings of tendon noted as tendon 2a and 2b from a branching point placed between joint 1 and the corresponding actuator. One of the divaricate tendons is attached the link that connect joint 1 and joint 2, and another is attached the end link. The motions of two joints of this manipulator are coupled by the geometric constraint generated by the branching tendon under the certain condition. In this section, we express the kinematics of manipulator with non-stretch branching tendon briefly, and derive the condition to keep the coupled motion of the two joints. In the tendon-driven manipulator, the representation of the relation between its joint angular velocities and its tendon displacement velocities is needed in addition to the general expression of the relation between its end-point velocity and its joint angular velocities to describe its kinematics. Given a vector of joint angular velocity $\dot{\boldsymbol{\theta}}$ and a vector of tendon displacement velocity $\dot{\boldsymbol{l}}$, the relation

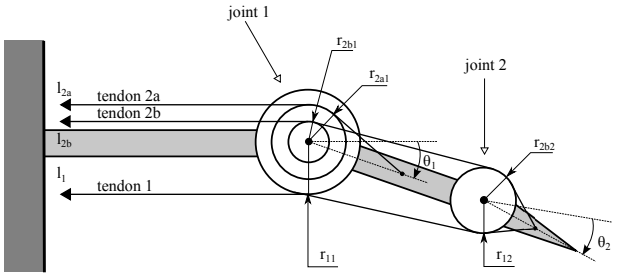

Fig. 2. Model of the proposed robotic finger regarding the branching tendon in the proposed robotic finger as independent two tendons.

between them are represented as follows:

$$\dot{\boldsymbol{l}} = \boldsymbol{P}\dot{\boldsymbol{\theta}}, \tag{1}$$

where $\boldsymbol{P}$ is called a tendon Jacobian matrix and determined by the routing of each tendon. The relation between tensile force of each tendon and each joint torque also can be represented using with $\boldsymbol{P}$ as follows:

$$\boldsymbol{\tau} = -\boldsymbol{P}^T\boldsymbol{f}, \tag{2}$$

where $\boldsymbol{\tau}$ is a vector of joint torque and $\boldsymbol{f}$ is a vector of tensile force. In the case of that the manipulator has tendons which number is larger than joints and $\boldsymbol{P}$ is a column full-rank matrix, using with the vector of joint torque, the tensile force vector is given as

$$\boldsymbol{f} = -\boldsymbol{P}^+\boldsymbol{\tau} + \boldsymbol{f}_b, \tag{3}$$

where $\boldsymbol{P}^+$ is a pseudo-inverse matrix of $\boldsymbol{P}$ and $\boldsymbol{f}_b$ is its null-space. $\boldsymbol{f}_b$ is called a bias tensile force. More details of the kinematics of general tendon-driven manipulator can be seen in Kobayashi et al.[10] or some textbooks of robotics[11, **?**]. Regarding the branching tendon in the proposed robotic finger as independent two tendons, the manipulator can be considered as a manipulator with three tendons as shown in Fig. 2. In this case, align (1) can be represented as follows:

$$\begin{bmatrix} \dot{l}_1 \\ \dot{l}_{2b} \\ \dot{l}_{2a} \end{bmatrix} = \boldsymbol{P} \begin{bmatrix} \dot{\theta}_1 \\ \dot{\theta}_2 \end{bmatrix}, \tag{4}$$

where l_i is each tendon displacement, and the tendon Jacobian matrix is given as:

$$\boldsymbol{P} = \begin{bmatrix} -r_{11} & -r_{12} \\ r_{2b1} & r_{2b2} \\ r_{2a1} & 0 \end{bmatrix}, \tag{5}$$

where r_{ij} is a moment arm between each tendon and each joint, and its subscript indicates the corresponding joint and tendon. Note that the positive rotation is in a counterclockwise direction in the figure and positive displacement of the tendon is in a pulling direction. In order to apply any desired torque to each joint, the system has to be tendon controllable depending on elements of the matrix $\boldsymbol{P}$[10]. We assume that $\boldsymbol{P}$ is satisfied the condition to be tendon controllable.

We consider the kinematics in the case that the manipulator has a branching tendon as Fig. 1 based on the expression described above. The branching tendon is sometimes used to realize the underactuated manipulator[**?**]. Sawada and Ozawa[12] proposed a generalized control method for tendon-driven mechanism with branching tendons. Shirafuji et al.[**?**] has been proposed that the tenodn-driven manipulator with branching tendons can be controlled as a manipulator with less DoFs than original DoFs virtually under the assumption that the branching tendon has no elasticity. It is caused by the geometric constraint of the branching tendon which generate coordinated motion of the joints. In addition, they implied that the system can be released arbitrarily from this coupled motion by adjusting the bias tensile force. We apply the method proposed by Shirafuji et al.[**?**] to the proposed robotic finger, and derive the condition to keep the coupled motion.

Shirafuji et al.[**?**] use a virtual tendon Jacobian matrix $\boldsymbol{P}_v$ to represent the relation between tendons include branching tendons and coupled joints. First, we derive this matrix of the proposed robotic finger. align (4) can be divided as follows:

$$\dot{l}_1 = \boldsymbol{P}_1 \begin{bmatrix} \dot{\theta}_1 \\ \dot{\theta}_2 \end{bmatrix}, \tag{6}$$

$$\begin{bmatrix} \dot{l}_{2a} \\ \dot{l}_{2b} \end{bmatrix} = \boldsymbol{P}_2 \begin{bmatrix} \dot{\theta}_1 \\ \dot{\theta}_2 \end{bmatrix}, \tag{7}$$

where $\boldsymbol{P}_1$ and $\boldsymbol{P}_2$ are the corresponding submatrices given as:

$$\boldsymbol{P}_1 = \begin{bmatrix} -r_{11} & -r_{12} \end{bmatrix} \quad \boldsymbol{P}_2 = \begin{bmatrix} r_{2b1} & r_{2b2} \\ r_{2a1} & 0 \end{bmatrix}. \tag{8}$$

If there is no slacked tendon, the tendon displacement velocities of two tendons branched from tendon 1 has to be same because they are connected at the same point. Therefore, $\dot{l}_{2a} = \dot{l}_{2b} = \dot{l}_2$ and align (7) can be rewritten as:

$$\dot{l}_2 \begin{bmatrix} 1 \\ 1 \end{bmatrix} = \boldsymbol{P}_2 \begin{bmatrix} \dot{\theta}_1 \\ \dot{\theta}_2 \end{bmatrix}. \tag{9}$$

The joint angler velocity is derived using the inverse of $\boldsymbol{P}_1$ as:

$$\begin{bmatrix} \dot{\theta}_1 \\ \dot{\theta}_2 \end{bmatrix} = \dot{l}_2 \boldsymbol{P}_2^{-1} \begin{bmatrix} 1 \\ 1 \end{bmatrix} = \frac{\dot{l}_2}{r_{2a1}} \begin{bmatrix} 1 \\ \frac{r_{2a1} - r_{2b1}}{r_{2b2}} \end{bmatrix}. \tag{10}$$

During the coupled motion under the assuming there is no slack, it can be seen that the relation between each joint angular velocity is described as:

$$\dot{\theta}_1 : \dot{\theta}_2 = 1 : \frac{r_{2a1} - r_{2b1}}{r_{2b2}}. \tag{11}$$

The condition not to cause slackness to tendons will hereinafter be described in detail. We define a virtual angle θ_v to represent the angle of coupled joints as $\dot{\theta_v} = \dot{l}_1$. Substituting align (10) into align (4), we obtain the follows:

$$\begin{bmatrix} \dot{l}_1 \\ \dot{l}_{2b} \\ \dot{l}_{2a} \end{bmatrix} = \begin{bmatrix} \boldsymbol{P}_1 \\ \boldsymbol{P}_2 \end{bmatrix} \dot{l}_2 \boldsymbol{P}_2^{-1} \begin{bmatrix} 1 \\ 1 \end{bmatrix} = \begin{bmatrix} \boldsymbol{P}_1 \boldsymbol{P}_2^{-1} \begin{bmatrix} 1 \\ 1 \end{bmatrix} \\ 1 \\ 1 \end{bmatrix} \dot{\theta_v}. \tag{12}$$

From the fact that $\dot{l}_{2a} = \dot{l}_{2b} = \dot{l}_2$ when there is no slack, align (12) can be rewritten as:

$$\begin{bmatrix} \dot{l}_1 \\ \dot{l}_2 \end{bmatrix} = \begin{bmatrix} \boldsymbol{P}_1 \boldsymbol{P}_2^{-1} \begin{bmatrix} 1 \\ 1 \end{bmatrix} \\ 1 \end{bmatrix} \dot{\theta_v}. \tag{13}$$

This align can be regarded as the relation between the joint angular velocities and the tendon displacement velocity of the tendon-driven manipulator with 1-DoF and two tendons. In this case, the tendon Jacobian matrix of the system is described as:

$$\boldsymbol{P}_v = \begin{bmatrix} \boldsymbol{P}_1 \boldsymbol{P}_2^{-1} \begin{bmatrix} 1 \\ 1 \end{bmatrix} \\ 1 \end{bmatrix}, \tag{14}$$

and we call $\boldsymbol{P}_v$ as virtual tendon Jacobian matrix. Second, we apply this matrix to align (2). Multiplying both sides of align (2) by $(\boldsymbol{P}_2^{-1}[1\ 1]^T)^T$, we obtain the follows:

$$\begin{bmatrix} 1\ 1 \end{bmatrix} \boldsymbol{P}_2^{-T} \boldsymbol{\tau} = - \begin{bmatrix} 1\ 1 \end{bmatrix} \boldsymbol{P}_2^{-T} \boldsymbol{P}^T \boldsymbol{f} = -\boldsymbol{P}_v \begin{bmatrix} f_1 \\ f_{2a} + f_{2b} \end{bmatrix}, \tag{15}$$

where f_i is each tensile force and $f_{2a} + f_{2b}$ is equivalent to the tensile force of the branching tendon f_2. Furthermore, defining virtual torque vector as:

$$\tau_v = \begin{bmatrix} 1\ 1 \end{bmatrix} \boldsymbol{P}_2^{-T} \boldsymbol{\tau}, \tag{16}$$

we can control the proposed robotic finger regarding as the tendon-driven manipualator with 1-DoF and two tendons virtually under the assuming that there is no slack of tendon.

We assumed that there is no slack of tendon in the above discussion, but the coupled motion is lost when one of the divided tendons is slack. This slack is caused by forces applied to the robotic finger, include external force generated

by the contact with the environment and inertial force during its motion. The proposed robotic finger has a branching tendon, and there are two states of tendons when slackness is occurred as shown Fig. 3. These states can be used when we wish to control the robotic finger without the coupled motion of joints (e.g. we wish to manipulate the grasped object using with the end link of the robotic finger). Finally, therefore, we derive the condition that one of the tendons divided from the branching tendon become slack when torques are applied to the joints as a result of the external force applied to the fingertip as shown in Fig. 4. We consider the planar motion, and given the external force vector $\boldsymbol{F}$ which is applied to the tip of robotic finger, the relation between the external force and joint torques can be represented as:

$$\boldsymbol{\tau} = \boldsymbol{J}^T \boldsymbol{F}, \tag{17}$$

where $\boldsymbol{J}$ is a Jacobian matrix representing the relation between velocity of the contact point in each direction and each joint angular velocity. Assuming the frictionless point contact, the external force vector can be described as $\boldsymbol{F} = [0\ F]^T$, and align (17) can be written as:

$$\boldsymbol{\tau} = \begin{bmatrix} L_1 \cos\theta_1 + L_2 \cos(\theta_1 + \theta_2) \\ L_2 \cos(\theta_1 + \theta_2) \end{bmatrix} F, \tag{18}$$

where L_1 is the length of the link between the joints and L_2 is the distance between the contact point and joint 2. The slack of each tendon is ocurred when its tensile force becomes negative because a tendon can not exert a pushing force. Therefore, substituting align (18) into align (3), we obtain the follows:

$$\begin{bmatrix} f_1 \\ f_{2b} \\ f_{2a} \end{bmatrix} = -\boldsymbol{P}^+ \begin{bmatrix} L_1 \cos\theta_1 + L_2 \cos(\theta_1 + \theta_2) \\ L_2 \cos(\theta_1 + \theta_2) \end{bmatrix} F + \boldsymbol{f}_b, \tag{19}$$

where we regard the branching tendon as independent tendons as shown Fig. 4. When one of f_{2b} and f_{2a} become negative for given the external force F and the bias force vector $\boldsymbol{f_b}$, the state of tendons change to the state such as Fig. 3, and this is the condition to nullify the coupled motion. We use these derived relations in this section to develop the robotic finger and validate the state transition of the tendons caused by the slack of tendon in the following section.

3 Development of robotic finger

We produced the robotic finger with branching tendon for developing the gripper. Finger has two DOFs in flexion/extension and is composed of three links and five pulleys.

Finger movement, such as fingertip trajectory and ratio of angles between coupled joints, can be fixed by the moment arms of each tendon. Therefore, the value of moment arm is important. Developed finger is driven by extension bifurcate tendon and flexion tendon. This arrangement of tendons is partly similar

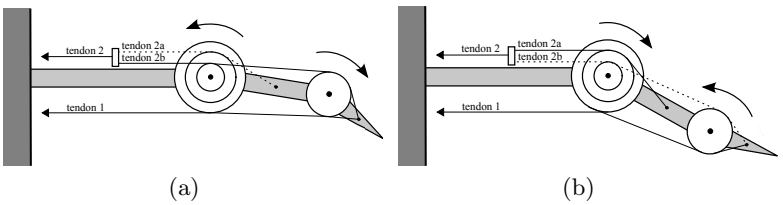

Fig. 3. States of the tendons when one of them is slack. The slacked tendon is illustrated as a dotted line. (a) The state when tendon 2a is slack. (b) The state when tendon 2b is slack.

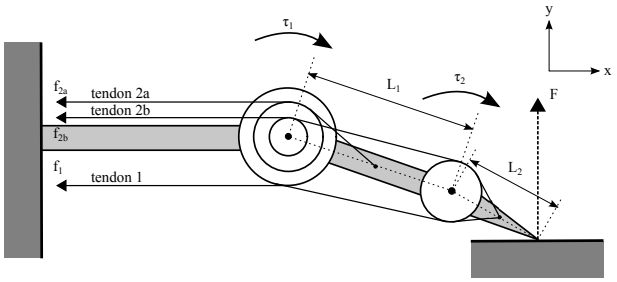

Fig. 4. Model of the equilibrium of force resulting from a contact with the environment.

to that of man's finger. Hence, we decided the moment arms with reference to that of man's finger which Leijnse et al.[13], Spoor[14] shows. Table 1 shows the value we use. According to Leijnse et al.[13], the moment arm r_{2b1} is represented as nonlinear function of PIP joint angle. However Shirafuji et al. reproduce this with arrangement of 2 pulleys, in this research, we chose constant as this moment arm for siumplicity. These moment arm are represented by the diameter of the pulleys in this design. In addition, the link lengths between the joints relate to fingertip force and finger trajectory. Table 2 shows this link lengths.

Table 1. Diameters of the pulleys[mm]

	tendon 1	tendon 2b	tendon 2a
joint 1	r_{11}	r_{2b1}	r_{2a1}
	7	3	5
joint 2	r_{12}	r_{2b2}	-
	4	4	-

Table 2. Lengths of links[mm]

parts	length
fingertip - joint 2	22
joint 2 - joint 1	30.5

Using these moment arms, this finger's tendon Jacobian matrix is defined and we can control the finger with the Jacobian. Also, the ratio between the

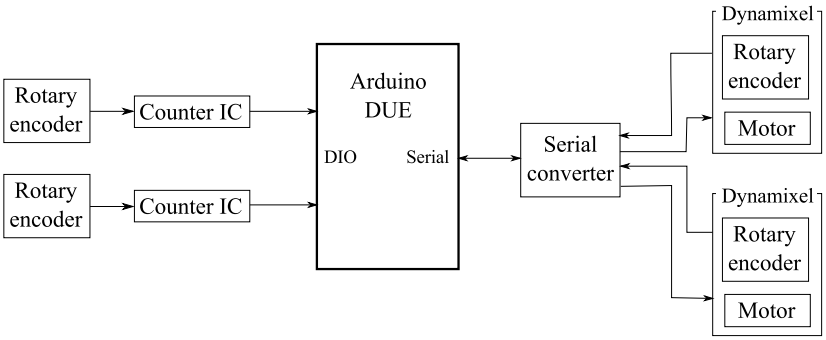

Fig. 5. Hardware system of the developed finger.

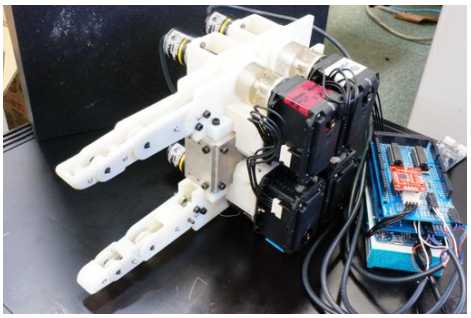

Fig. 6. Exterior of the developed finger.

changes in the joint angle vector shown by Eq.10 is calculated as follows:

$$\dot{\theta_1} : \dot{\theta_2} = 1 : \frac{r_{2a1} - r_{2b1}}{r_{2b2}} = 1 : \frac{1}{2}$$

We constructed control system of finger. Fig.5 shows composition of control system, and Fig.6 shows the exterior of finger system. Each tendons of finger is driven by servo motors(Dynamixel MX-64R),and the rotation angle of a base pulley which wind the tendon, is measured by rotary encoder(OMRON E6A2-CW3C). Tendon displacement can be calculated with this angle. And, the output pulses of encoder are counted by counter IC(NEC μ PD 4702C). The finger is controled by Arduino DUE using these component. Arduino gives any instructions to servo motors, reads the value of counter, and calculate variables used for control of finger.

On this tendon-driven finger, tensile force $\boldsymbol{f}$ and tendon displacement velocity $\dot{\boldsymbol{l}}$ is controled by winding tendon wire round base pulley. Base pulleys are not directly connected servo motors, but driven by torque of linear torsion springs which are put between servo motors and base pulleys. Torque which spring exerts can be calculated using displacement of spring which is obtained by angles of

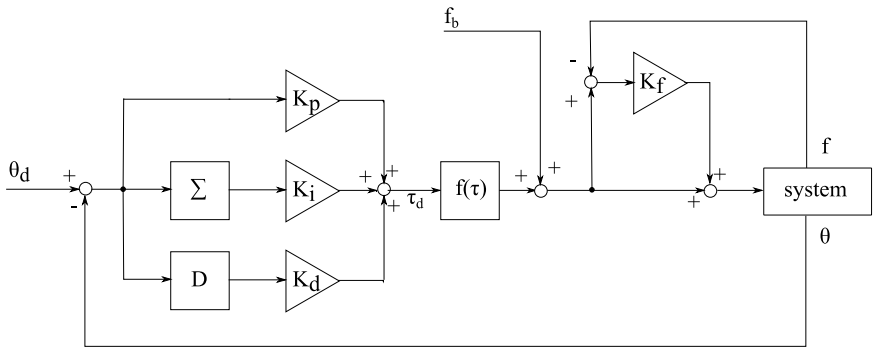

Fig. 7. Image of position control system

servo and base pulley. This torque is brought close to the target torque by control system. We equipped the finger with torsion springs having a spring constant of 5.17N/mm. The rotary encoders which measure angles of base pulley are directly connected shafts of base pulley. In experiments of this developed finger, we don't have to make the finger fast movement. Therefore, encoder's shaft doesn't make fast rotation, recieve large radial and thrust load, we think.

While each tendon, including branched tendon, have no slack, finger's angular position and fingertip force can be controled by composed system. Fig.7 shows the image of position control system implemnted finger. This control is discrete system and micro computer on Arduino repeats this chain of calculation. In figure, D reveals differentiator and S is integrator. The angular position control uses PID. And current torque of spring is fed back to target torque calculated in position control loop. Restricting finger movement on horizontal plane, gravity compensation is not included in the system. When not needing position control, finger can move with only feedback control of spring torque, giving the value of joint torque which exerts target fingertip forces.

Fig.8 shows tracking performance of developed system. We look up delay of initial response in the graph. This can be caused by rotational friction of joints on not the shaft but the surface of finger frame. In this time, we didn't sufficiently configulate each gain constant because position control is not main focus in this research. If we had to improve responsibility, we can configure gain.

4 Validation of tendon slack

Developed robotic finger can make slack one of the branched tendon, depending on the condition of both bias tensile force of all tendons and fingertip force exerted. We validated whether finger in real environment move along the theory which we shows previous section with developed finger.

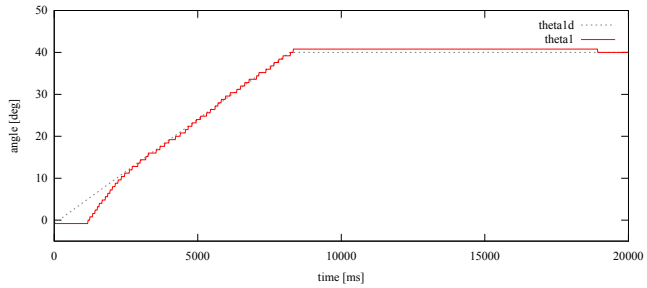

Fig. 8. Transition of target angle and real angle calculated from the value of tendon displacement of joint 1 when controled position

In order to make tendons of the finger slacken, either value of tensile force of tendon 1s or 1p which is calculated by Eq.19 have to become negative. Using $\theta_1 = 2\theta_2$ and the tendon Jacobian $\boldsymbol{P}$ derived from the moment arms represented in Table 1, Eq.19 is defined as follows:

$$\begin{bmatrix} f_1 \\ f_{2b} \\ f_{2a} \end{bmatrix} = \begin{bmatrix} 0.0606L_1 \cos 2\theta_2 + 0.1098L_2 \cos 3\theta_2 \\ 0.0606L_1 \cos 2\theta_2 - 0.1402L_2 \cos 3\theta_2 \\ -0.1515L_1 \cos 2\theta_2 + 0.0387L_2 \cos 3\theta_2 \end{bmatrix} F + \begin{bmatrix} 1 \\ 1 \\ 0.8 \end{bmatrix} f_b, \qquad (20)$$

where f_b is a bias tensile force variable.

When F and θ_2 is fixed, the value of f_b which make f_{1p} or f_{1s} to zero is calculated. When f_b fall short of this value, tensile force of one of the branch get minus and that branch slacken. Fig.9 shows this value of f_b against θ_2 or F. As figure shown, on the developed finger, the value of f_b which make f_{1s} to zero

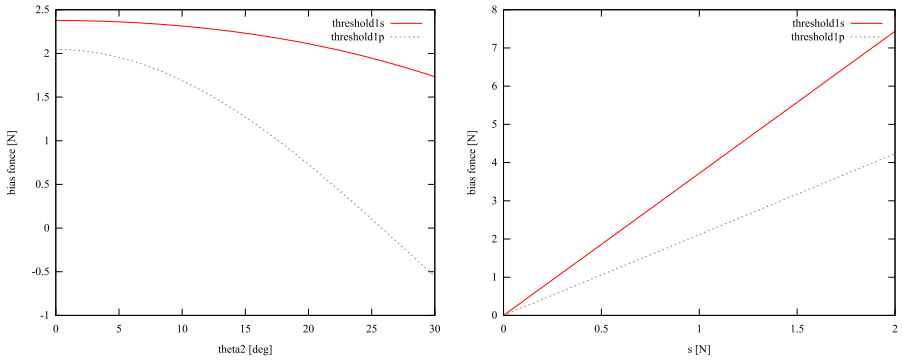

(a) Limit of f_b against θ_2 when $F = 0.6$ (b) Limit of f_b against F when $\theta_2 = 15°$

Fig. 9. Limit value of f_b to keep f_{2a} or f_{2b} positive

is larger than that of f_{1p} in any θ_2, s. Therefore, f_{1s} fall to zero and tendon 1s

loosen before f_{1p} do, while gradually lowering f_b. In order to make tendon 1p slack, we have to change moment arms which defined the values of the matrix $\boldsymbol{A}$. This change need to produce new pulleys bacause the moment arms represented by the diameter of pulleys on joints.

We experimented to validate level of agreement the theory and real movement. Fig.10 shows the appearance of experiment. According to the previous

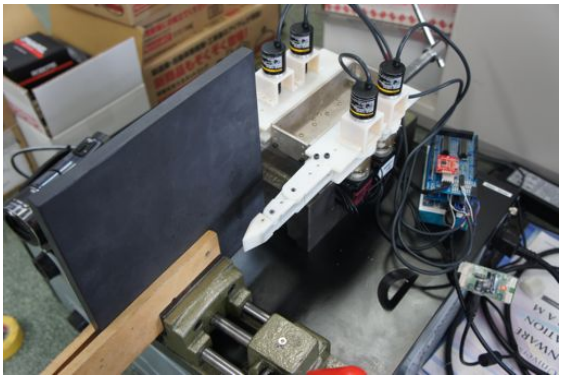

Fig. 10. Appearance of experiment

discussion, the value of f_b to loosen the tendon depends on joint angles and fingertip force. We experimented as follows:

1. Stabilize the unbent finger with large f_b enough to keep joints coupling.
2. Cntrol the finger with the tendon tensile force corresponding the joint torques which can generate a certain fingertip force F.
3. Hit the finger against the fixed low-friction board with a certain joint 2 angle θ_2.
4. Gradually decrease f_b.
5. Observe the value of f_b at the moment when tendon 2a loosen.

Here, when the ratio of bias force between tendon 2 and tendon 1 is $1 : 1.8$, bias force can't generate the joint torques and finger doesn't move. However, practically, finger movement occured when we set this ratio and actuate finger. This is caused by various factor such as difficulty to set initial displacement of torsion spring to zero. Then, before starting experiment, we stabilized finger with some bias force at the point where finger is extended in a straight line. We use the ratio of tendon 1 tensile force to tendon 2 in this time as the ratio of bias force.

The result obtained by actuation of finger using $\theta_2 = 15°$ as joint angle and $s = 0.6, 0.8$ as fingertip force is shown in Fig.11. In addition, an example of finger movement in the experiment is shown in Fig.12. In Fig.11, "bias force" represents the value of f_b in Eq.20 and this is bias force of tendon 2. "encoder

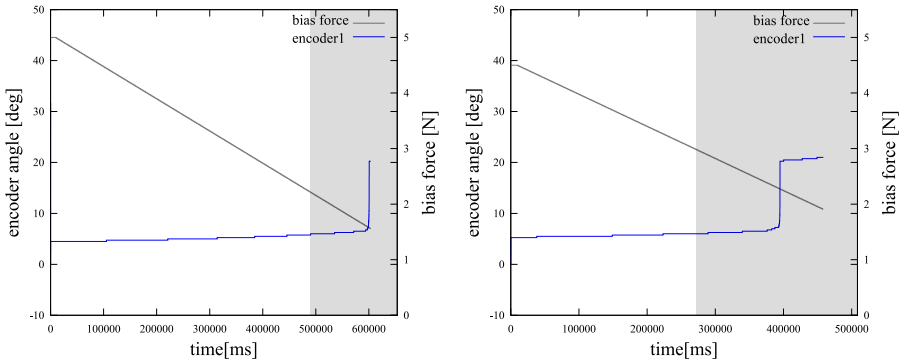

(a) $s = 0.6$ (b) $s = 0.8$

Fig. 11. Result of experiment$\theta_2 = 15°$

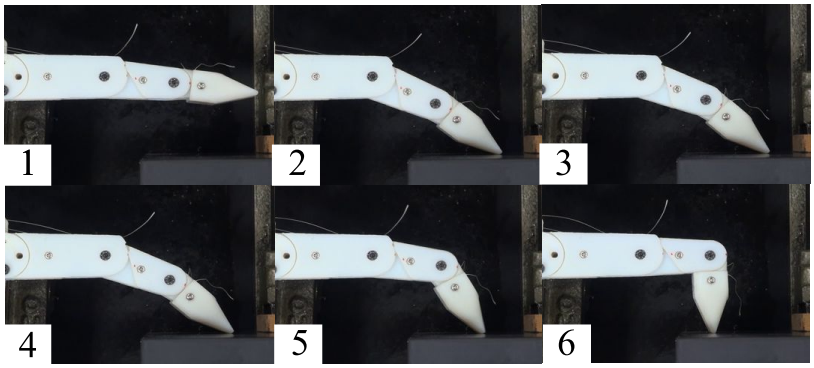

Fig. 12. Example of finger movement in the experiment. After the bias tensile force f_b fall short of the limit, figer move.

angle" represents the angle deplacement of the drive shaft measured by the rotary encoder which drive tendon 1. The area painted gray is which mathematically tensile force of tendon 1s is minus. As graph shows, tendon1s get slack and finger movement causes increasement of the value of the encoder after bias tensile force f_b fall short of the limit to keep tendon 1s's tensile force positive. It is verified that the slack of one of the branching tendon is caused by the value of bias tensile force.

The value which practically finger movement started is smaller than the calculated value for loosning tendon 1s. We can consider that the main reason of this gap is the factor we ignored in the derivation of the condition to loosen tendon or the real environment. As the main factor we disregarded, we mention the sliding friction between the fingertip and the board and the rolling friction on the joints. If we notes the effect of these friction, finger's shape change need

not only slack of tendon but also large force enought to get over the frictions. Then, finger movement come later than tendon relax. In the experiment, we could observe loosening tendon shortly before finger slided. Hence, when we control the finger, it is needed to consider these derived from dynamics of the robot. Moreover, the difficulty to adjust the ratio of bias tensile force possibly affect the diffrence. This ratio changes and is not clearly decided because of joint friction and setting initial position of torsion spring. We need to reduce the effect of these problem with improvement of robotic finger.

In addition, the measurement error on link lengths and joint angles also affects. For example, if a shorter length than that of the real finger uses, the value of bias tensile force to loosen tendon is calculated larger than the actual. At the same time, the actual fingertip force is smaller than expected because the joint torque to exert the requested force is calculated smaller. The smaller fingertip force, the smaller the value necessary for slacking off tendon. Therefore, the shorter measured length than the actual, the larger the difference between calculated and real bias tensile force to loosen branch.

5 Conclusion

We presented our two joint robotic finger which has branching tendon. First, we produced and actuated the finger system with position and tensile force control. Second, we found the condition to loosen branched tendon in the situation like that the finger exert a vertical force at the fingertip against a plane surface. We validated this condition of bias tensile force using the developed finger system. As a result, there is some gap between the calculation and the value to make the tendon slacken which is observed in the experiment. Though, we could expect the reasons about this diffrence as like above discussion and intentionally loosen the branch. This result can be an indication to actuate fingers of a gripper having a branching tendon with slack of branches.

In this paper, we can't deal with a gripper with the developed finger. We need to consider and investigate about a grasping tactics, a control of a gripper, and so on. It is expected that nonelastic branching tendon mechanism become a notable factor on the field of robotic, especially anthropomorphic hand. In the future, further study about this mechanism is required.

References

1. Salisbury, J., Craig, J.: Articulated hands: Force control and kinematic issues. The International Journal of Robotics Research **1**(1) (Mar. 1982) 4–17
2. Jacobsen, S., Iversen, E., Knutti, D., Johnson, R., Biggers, K.: Design of the utah/mit dextrous hand. In: Proceedings IEEE International Conference on Robotics and Automation. (Apr. 1986) 1520–1532
3. Butterfass, J., Grebenstein, M., Liu, H., Hirzinger, G.: Dlr-hand ii: Next generation of a dextrous robot hand. In: Proceedings IEEE International Conference on Robotics and Automation. (2001) 109–114

4. Vande Weghe, M., Rogers, M., Weissert, M., Matsuoka, Y.: The act hand: design of the skeletal structure. In: Proceedings IEEE International Conference on Robotics and Automation. (Apr. 2004) 3375–3379
5. Birglen, L., Gosselin, C., Laliberté, T.: Underactuated robotic hands. Volume 40. Springer Verlag (2008)
6. Hirose, S., Umetani, Y.: The development of soft gripper for the versatile robot hand. Mechanism and Machine Theory **13**(3) (Jan. 1978) 351–359
7. Kaneko, M., Higashimori, M., Takenaka, R., Namiki, A., Ishikawa, M.: The 100 g capturing robot-too fast to see. Mechatronics, IEEE/ASME Transactions on **8**(1) (2003) 37–44
8. Fukaya, N., Asfour, T., Dillmann, R., Toyama, S.: Development of a Five-Finger Dexterous Hand without Feedback control: the TUAT/Karlsruhe Humanoid Hand. In: Proceedings of the IEEE/RSJ International Conference on Intelligent Robots and Systems. (2013) 4533–4540
9. Shirafuji, S., Ikemoto, S., Hosoda, K.: Development of a tendon-driven robotic finger for an anthropomorphic robotic hand. The International Journal of Robotics Research (2014) in press.
10. Kobayashi, H., Hyodo, K., Ogane, D.: On tendon-driven robotic mechanisms with redundant tendons. The International Journal of Robotics Research **17**(5) (May 1998) 561–571
11. Murray, R., Li, Z., Sastry, S.S.: A mathematical introduction to robotic manipulation. CRC Press (1994)
12. Sawada, D., Ozawa, R.: Joint control of tendon-driven mechanisms with branching tendons. In: Proc. IEEE Int. Conf. Robot. Autom. (May 2012) 1501–1507
13. Leijnse, J., Kalker, J.: A two-dimensional kinematic model of the lumbrical in the human finger. Journal of Biomechanics **28**(3) (Mar. 1995) 237–249
14. Spoor, C.: Balancing a force on the fingertip of a two-dimensional finger model without intrinsic muscles. J. Biomech. **16**(7) (1983) 497–504